Journal of Insect Physiology 149 (2023) 104547

Contents lists available at ScienceDirect

Journal of Insect Physiology

journal homepage: www.elsevier.com/locate/jinsphys

The tracheal system of the Common Wasp (Vespula vulgaris) – A micro-CT study

G.D. Bell [a], N. Corps [a], D. Mortimer [b], S. Gretton [a], N. Bury [a], G.J. Connett [c,*]

[a] School of (EAST) Engineering, Arts, Science and Technology, University of Suffolk, James Hehir Building, University Avenue, Ipswich, Suffolk IP3 0FS, UK
[b] Newbourne, Woodbridge IP12 4NR, UK
[c] National Institute for Health Research, Southampton Biomedical Research Centre, Southampton Children's Hospital, UK

ARTICLE INFO

Keywords:
Micro-computer tomography
X-ray
Micro CT
Vespula vulgaris
Queen and worker wasps
Tracheal system
Diagnostic radioentomology

ABSTRACT

X-ray micro-CT has been used to study the tracheal system of Pre and Post hibernation Queen wasps (Vespula vulgaris) and their workers. We have compared our findings in wasps with Snodgrass's description of the tracheal system of the honeybee as characterised by anatomical dissection. Our images, whilst broadly similar, identify the tracheal system as being considerably more complex than previously suggested. One of the 30 wasps imaged had a markedly different, previously undescribed tracheal system. Since completing this study, a large micro-CT study from the American Museum of Natural History (AMNH) has been published. This used different software (Slicer) and analysed 16bit digital data. We have compared our methods with that described in the AMNH publication, adopted their suggested nomenclature and have made recommendations for future studies.

1. Introduction

An extensive and comprehensively referenced paper on the insect tracheal systems of Apterygotes, Paleoptera and Polyneoptera was recently published by the American Museum of Natural History (Herhold et al., 2023). The authors explain, that with few exceptions, (some Protura, Collembolola and Chironomid larvae), all insects examined thus far possess tracheae. These are epidermal invaginations that extend into the body and branch into ever finer tracheae and tracheoles and thus provide tissues direct access to air for gas exchange (Herhold et al., 2023).

One of the first detailed anatomical descriptions of the tracheal system was by Vinal who depicted the respiratory system of the Carolina locust, Dissosteira carolina (Vinal, 1919). His paper referenced the work of early pioneers such as the illustration of the respiratory system of the silkworm by Malpighi in 1669, the goat moth Cossus by Lyonet in 1762, and the cockchafer, Melolontha vulgaris by Strauss-Durckheim in 1828. Many more recent textbooks and papers on insect anatomy and physiology have acknowledged the excellent anatomical depictions of the honeybee's tracheal system by Snodgrass (1956) which was based on his meticulous multiple dissections.

Most tracheal studies highlight the difficulties in handling, dissecting, and processing extremely small and delicate tracheae and air sacs. It is frequently pointed out that air sac anatomy is highly susceptible to being distorted during dissection and it is impossible not to cut across extremely small tracheae within muscle and visceral tissues. Alternative methods to demonstrate tracheal anatomy, such as direct injection of dyes into the tracheal system (Wigglesworth, 1950), and corrosion casting with subsequent scanning electron microscopy (Meyer, 1989), have been attempted to overcome these limitations with limited success. More recently, the use of X-ray Synchrotron imaging has been a major advance (Westneat et al., 2003; Hartung et al., 2004; Kaiser et al., 2007; Greenlee et al.,2009; Greco et al., 2012; Kirton et al., 2012; Socha et al., 2013), but sufficient access to such imaging facilities has been a limiting factor for entomologists using and developing this modality. Despite such developments, and the use of more refined stereomicroscopic imaging capabilities, accurately characterising the anatomy and size of insect tracheal systems has until relatively recently been difficult and challenging.

More recently, the use of X-ray micro-CT techniques has enabled more detailed imaging of insect airway anatomy without tissue destruction (Friedrich and Beutel, 2008; Snelling et al., 2012; Shaka et al., 2013; Greko et al., 2014; Ivan et al., 2015; Alba-Tercedor, 2018; Herhold et al., 2023). In this paper we have explored the use of a modified X-ray micro-CT method to study the tracheal system of the common wasp, Vespula vulgaris. To our knowledge this insect's

* Corresponding author.
E-mail address: Gary.connett@uhs.nhs.uk (G.J. Connett).

https://doi.org/10.1016/j.jinsphys.2023.104547
Received 25 January 2023; Received in revised form 28 June 2023; Accepted 7 July 2023
Available online 13 July 2023

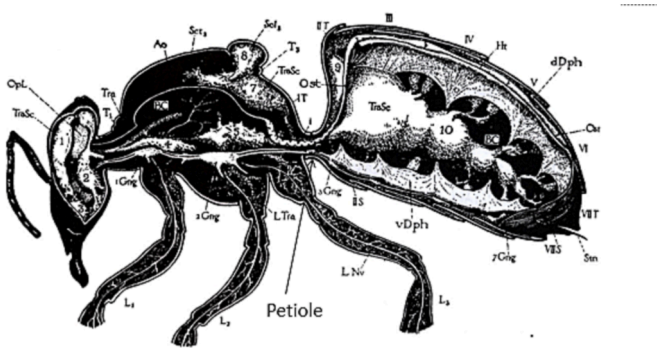

Fig. 1a. Sagittal midline illustration of a honeybee dissected and drawn by Snodgrass taken from Fig 78 of the 1956 print of his book. Snodgrass designated the air sacs in the head as 1–3 those in the thorax as 4–8 and those in the abdomen as 9 and 10. The narrow 'wasp's waist' or Petiole of the bee is shown by the black arrow. Used by permission of the publisher, Cornell University Press.

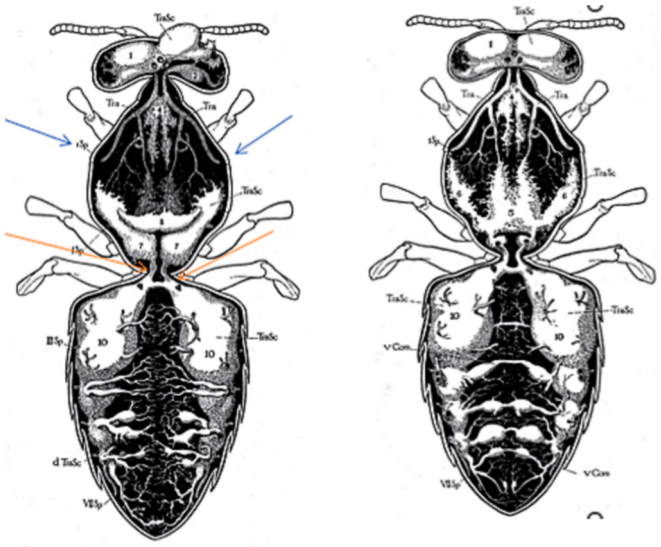

Fig. 1b. On the left is a dorsal cut-plane drawing of a honeybee dissected and drawn by Snodgrass taken from Fig 86 of the 1956 print of his book. Air sacs designated as 1,2,4,7,8 and 10 are labelled. A single pair of tracheal trunks are seen passing from the first thoracic spiracles (Sp I- blue arrows) forwards and down through the anterior thorax traversing the neck of the bee and supplying air sacs in the head. The two petiolar tracheal trunks (red arrows) pass forward into thoracic sacs 7 and 8 as well as caudally into the two large abdominal sacs (10). On the right is a more ventral, dorsal cut- plane drawing of a honeybee. A single pair of tracheal vessels are drawn passing from Sp I through the neck and into the head. The two petiolar tracheal trunks are drawn connecting with air sacs 5 and 6 in front and with abdominal air sacs 10 behind. Used by permission of the publisher, Cornell University Press. (For interpretation of the references to colour in this figure legend, the reader is referred to the web version of this article.)

respiratory system has not been studied in detail despite there being excellent accounts of most other aspects of its anatomy and life cycle (Duncan, 1939; Spradbery, 1973; Sumner, 2022).

2. Materials and methods

2.1. The wasps

Nine pre-hibernation and 12 post-hibernation queen Vespula vulgaris wasps were collected in Beccles, Suffolk, UK, as were five of ten worker wasps of the same species. The other five worker wasps were collected in Newbourne near Marlow on Thames, UK. The pre-hibernation queens (preQWs) were collected between late September and early November 2020 and the post- hibernation queens (postQWs) were caught in April-May 2021. The first five worker wasps (WWs) were caught in late 2020 and the second five in late August/early September 2021. All wasps appeared healthy and were actively flying when captured.

Soon after capture the wasps were killed and preserved by placing them in a domestic deep freezer at minus 20 degrees centigrade. They were then transferred to the Suffolk University's minus 80 degrees centigrade freezer as soon as possible for longer term storage. Wasps were removed from the freezer approximately 20 min prior to scanning

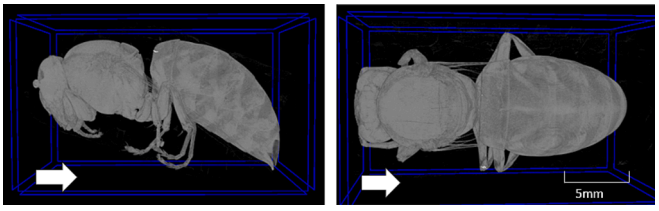

Fig. 2a. Two micro-CT 3-D volume views of Pre-hibernation Queen Wasp 1 (PreQW1). On the left is an external left lateral view and, on the right, an external dorsal view. The total length of PreQW1 was 18.5 mm. The solid white arrow on this and subsequent figures indicate an anterior to posterior direction. A 5 mm scale bar is shown.

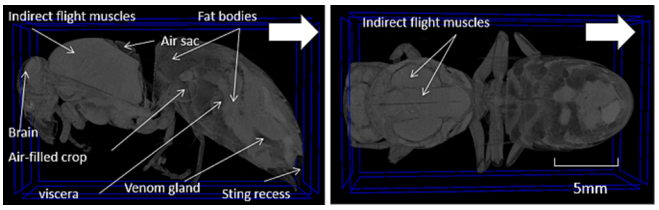

Fig. 2b. Cut-plane 3-D volume views of PreQW1 in midline sagittal and dorsal cut-plane views. The more radio-opaque structures such as the brain, skeletal muscles and viscera are whitest. Less radio- opaque structures, such as abdominal fat bodies and venom gland are relatively darker. The least radio-opaque air-filled structures such as the air sacs and the sting recess, and the surrounding air, show varying degrees of blackness. A 5 mm scale bar is shown.

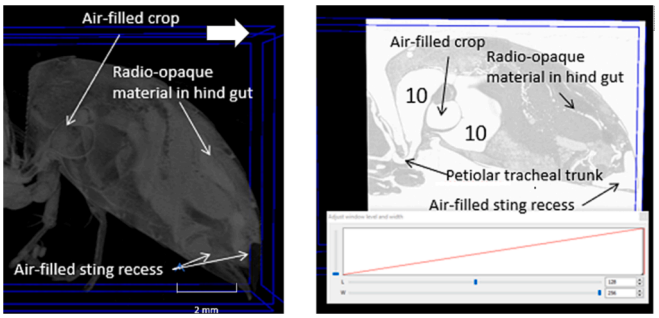

Fig. 3a. Two midline sagittal cut-plane 3-D volume of the abdomen of PreQW1. On the left is a view like Fig. 2b. On the right the stored X-ray attenuation values have been inverted from 0 to 255 to 255–0. At the default level windows settings of 128/255 the low attenuation tracheae, air sacs and other air-filled structures, including the surrounding air and air in the crop and sting recess, now appear brilliantly white while the previously most radio-opaque structure (which is the hind gut) now appears blackest. The large abdominal air sacs (10) that were obscured by low attenuation fat bodies in the conventional X-ray are now easily seen as is one of the two large tracheal trunks passing through the Petiole. The graph in the lower part of the figure is a histogram showing the default level (L) and width (W) when the inverted attenuation values are opened in the DISECT software. A 2 mm scale bar is shown.

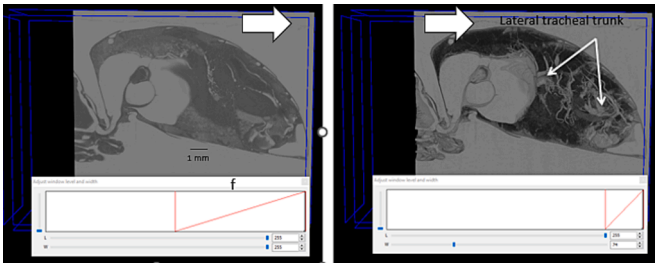

Fig. 3b. This shows the same midline sagittal 3-D volume cut-plane views of the abdomen of PreQW1 as shown in Fig. 3a but with the level/window settings altered to 255/255 on the left and 255/74 on the right. The large amount of low attenuation fat body tissue that was obscuring the right lateral longitudinal tracheal trunk and its various branches that pass ventrally, dorsally and to the viscera is no longer a factor. The scale bar in this and all subsequent figures is 1 mm.

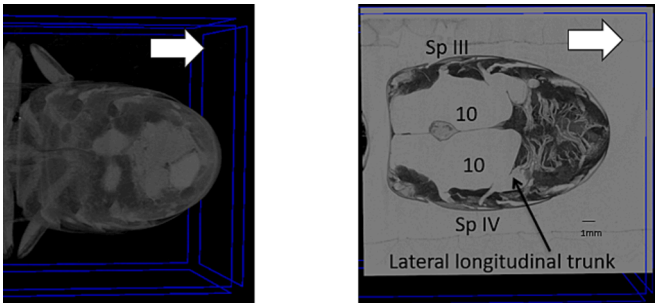

Fig. 3c. Two dorsal 3-D cut-plane views of the abdomen of PreQW 1. On the left is the 'normal' X-ray appearance and on the right the effect of inverting all the individual attenuation values and then adjusting the Level/Window settings to 255/74. Several of the spiracular tracheal trunks can be seen and, as in Fig. 3b, the two large abdominal air sacs designated as 10 by Snodgrass are clearly seen as are much of the two lateral longitudinal tracheae connecting the spiracular tracheae of spiracle III to VII.

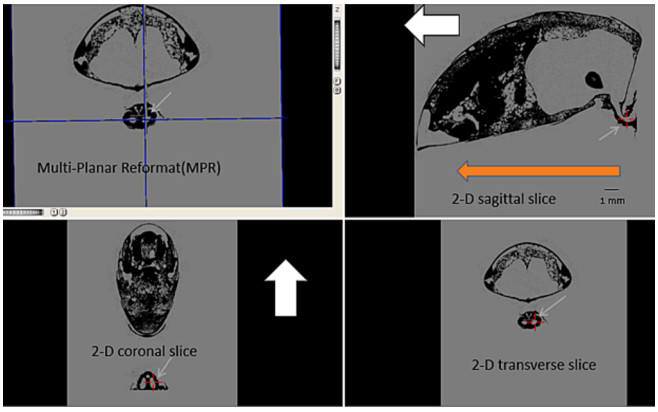

Fig. 4a. The top left image shows the use of the Multiplanar Reformat feature (MPR) in the Disect software in combination with the inverted 2-D sagittal, coronal, and transverse slice views of the abdomen of PreQW 1. The red cross hairs (white arrows) are placed over one of the two main tracheal trunks traversing the Petiole. The relevant slider is moved horizontally in the direction shown by the large orange arrow noting which white tracheal trunks and/or air sacs interconnect. In this figure and the next 3 figures the MPR views are shown at a Level and Window setting of 255/255. (For interpretation of the references to colour in this figure legend, the reader is referred to the web version of this article.)

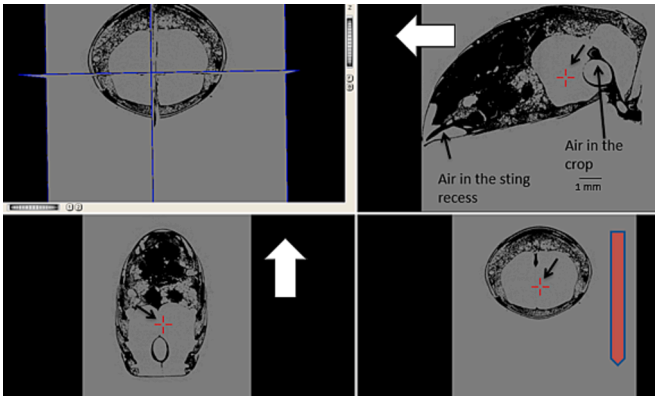

Fig. 4b. This shows a similar view to Fig. 4a, but the slider has been moved in the direction of the large red arrow so that the red cross hairs are now situated in the midline between the two main large abdominal air sacs (black arrows).

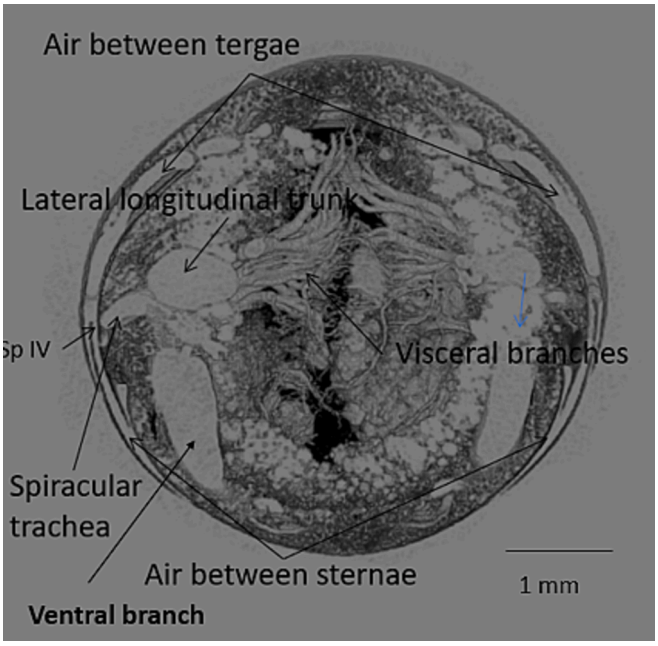

Fig. 5a. An inverted 3-D cut-plane transverse view through the abdomen of PreQW1 at the level of spiracle IV showing the spiracular trachea, the lateral longitudinal trunk, and its branches. Air trapped between individual overlapping tergae and sternae can superficially look like tracheal vessels (black arrows).

and allowed to thaw to room temperature. Wasps scanned in a SkyScan 1072 scanner were immobilised in cut-away plastic pipettes (VWR European Cat 129–0296 150 X 0.05 mm) surrounded with air with, if necessary, small pieces of dental wax gently packed around to ensure complete immobilisation of the sample. Wasps scanned in a SkyScan 1172 scanner were in air and immobilised using polystyrene foam mounts.

2.2. Micro CT imaging

The first five wasps (three post-hibernation queen wasps and two worker wasps) were scanned using a SkyScan 1072 desktop micro-CT scanner (Bruker-micro-CT, Kontich, Belgium) using a 180- degree rotation with 0.4-degree rotation step and 2X frame averaging. All five scans were performed at 70 kV and a filament current of 100μA. No aluminium filter was employed. Each scan took 75 min. The scans were

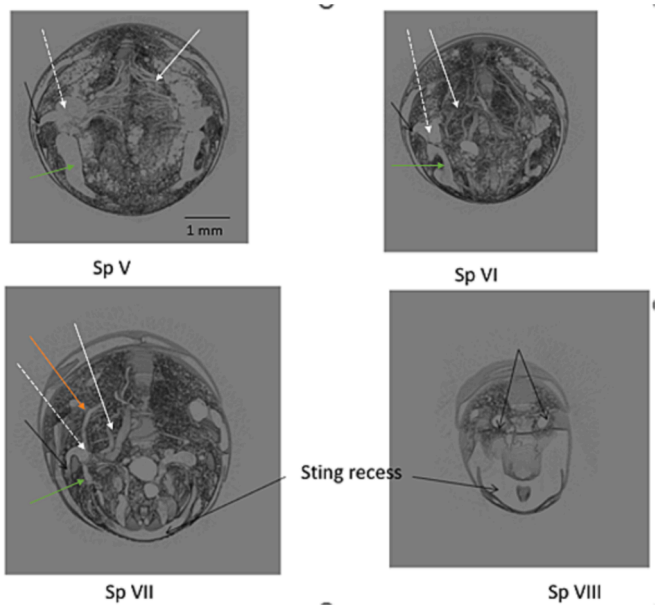

Fig. 5b. A series of transverse 3-D cut-plane views of the same wasp at the levels of the spiracular trunks of spiracles V-VIII (black arrows). The dotted white lines show the lateral longitudinal trunks, the orange, green and white arrows indicate respectively dorsal, ventral, and visceral branches arising from it. The air in the sting recess is also shown. (For interpretation of the references to colour in this figure legend, the reader is referred to the web version of this article.)

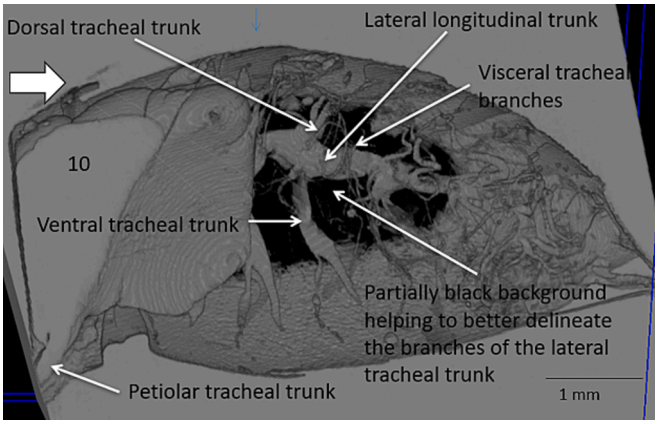

Fig. 6. An inverted cut-plane 3-D sagittal view of a worker wasp's abdomen. Although the whole of the lateral longitudinal tracheal trunk and its branches can be seen on a single midline sagittal cut- plane, it is possible to obtain a clearer view by performing a second parasagittal cut plane lateral to the tracheal trunk to produce a partially black background.

all performed isotropically at interpixellar distances varying from 26 down to 8.83 μm depending on specimen size. Each day before starting to scan a flat field correction was performed (Tarplee and Corps, 2008). The data were saved as 16-bit data. The remaining nine PreQWs, nine PostQWs and eight WWs were scanned using a more modern Skyscan 1172 micro-CT scanner (Bruker-micro-CT, Kontich, Belgium). These scans were all made at an isotropic interpixellar distance of 7.43 μm employing a 180-degree rotation with 0.4-degree rotation step and 2X frame averaging at 59Kv and a filament current of 167 μA. No aluminium filter was employed. Each scan took 23 min 15 s to perform. All images were saved as TIFFs at a depth of 16.

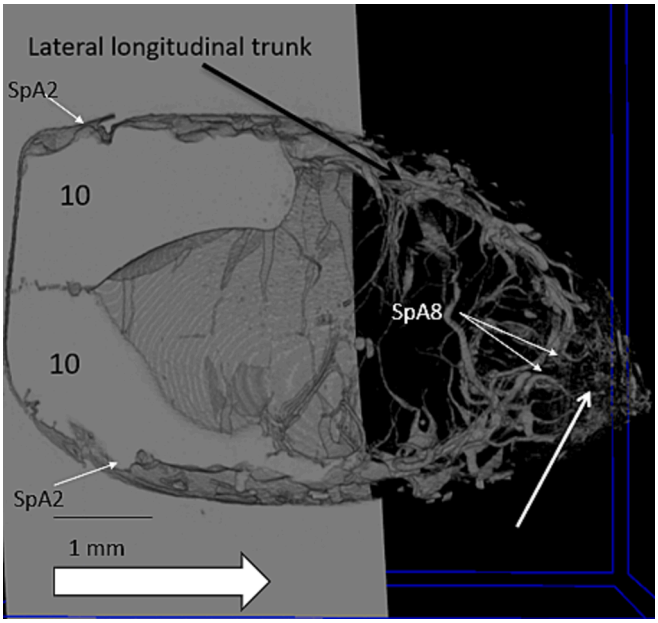

Fig. 7a. The 3-D cut-plane dorsal view of the abdomen of the worker wasp shown in Fig. 6. Half of the individual transverse 2-D slices have had most of the unwanted surrounding white areas removed. The larger white arrow points to the sting recess which still has a small amount of white material needing to be removed using 3-D Paint. The small white arrows on the left indicate the sites of entry of abdominal spiracles A2. The Abdominal spiracles A8 are within the sting recess and shown by the 2 right-sided small white arrows. The black arrow points to the lateral longitudinal trunk.

2.3. Reconstruction and beam hardening correction

Cone-beam reconstruction was carried out using NRecon 1.6.9.8 (Bruker-micro-CT, Kontich, Belgium). For the Skyscan 1072 studies we used a Gaussian smoothing value of 2, a ring artefact reduction value of 12 and a beam hardening correction value of 40. For the 1172 scans we used the same smoothing setting but a ring artefact correction of 10 and a beam hardening correction value of 50. Although the data were originally collected as 16bit data, we elected to reconstruct the images as 8-bit data as the file sizes were smaller and more manageable for both storage and data transfer.

2.4. Analytical software and X-ray attenuation inversion technique used

We used a combination of the software Disect (Tam et al., 2007; Bell et al., 2012;Greco et al., 2014; Thielens et al., 2018; Bell et al., 2020; Bell et al., 2021; Bell et al., 2023) and the very similar Skyscan viewing software consisting of Data Viewer (2D views) and/or CTVox (3D views) (both from Bruker microCT Kontich, Belgium). These different software packages were used to initially view the images of the entire wasps either as 2D slices in the transverse, sagittal or coronal planes, or as 3D volume views, cut plane 3D views, Maximum Intensity Projections (MIPs), or Multi-Planar Reconstructions (MPRs). These results were collected as 8-bit data and so X-ray attenuation values ranged from Completely black = 0 to intensely white = 256.

Since we could find no previous detailed description of the respiratory system of a wasp, even in monographs describing other organ systems (Duncan 1939; Spradbery, 1973), we elected to use as a 'road map' the well-known illustrations of Snodgrass based on his own meticulous dissections of the honeybee carried out in the early 1900s. These drawings are reproduced in several editions of his books including the 1956 and 1984 editions and are shown in Figs. 1a and 1b.

Having initially viewed each whole wasp micro-CT scan using both the 3-D volume and cut-plane facilities within Disect, (Fig. 2a and

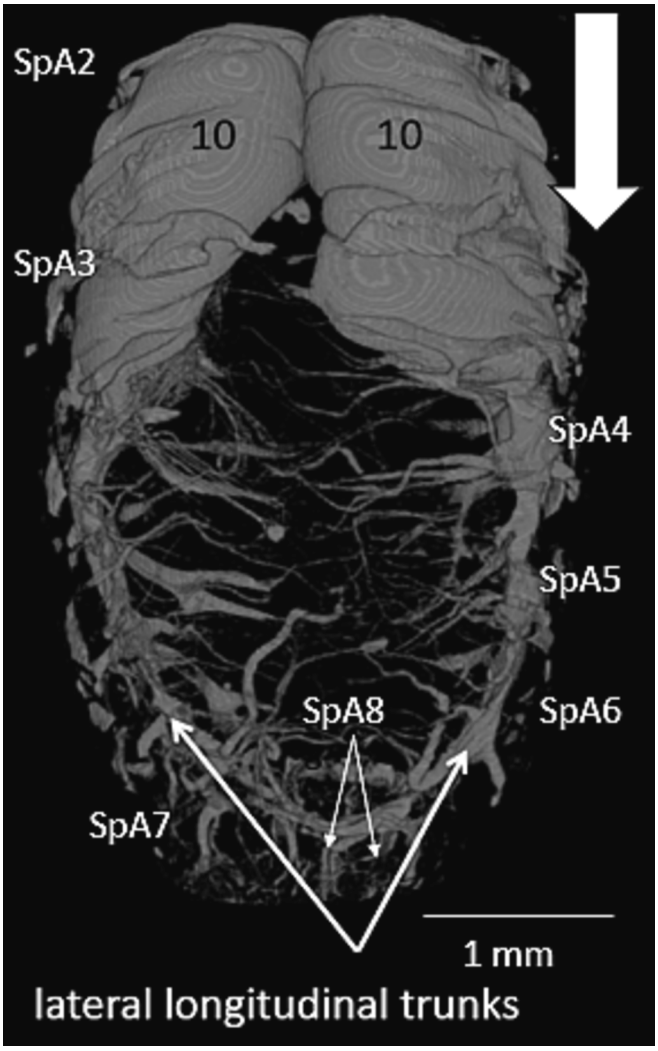

Fig. 7b. This shows the external 3-D volume appearance of the entire abdominal tracheal system after all the 2-D transverse slices have been processed using the same worker wasp as shown in Figs. 6 and 7a. The entry points of abdominal spiracles A2-A8 are shown.

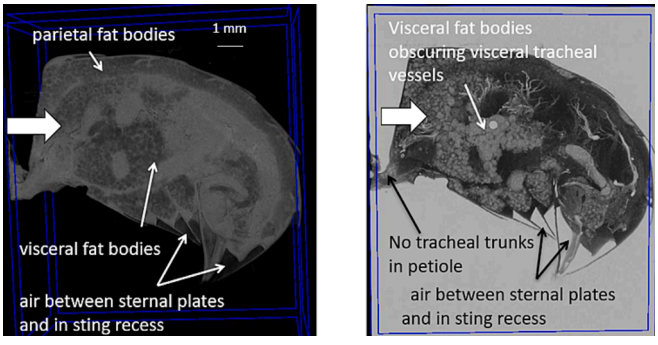

Fig. 8a. On the left is a normal 3-D cut-plane sagittal X-ray image of the abdomen of pre-hibernation queen wasp 8 (PreQW8). On the right is the same view after X-ray attenuation values have been inverted. The two large tracheal trunks that normally pass through the petiole are missing as are the two abdominal air sacs (10). The queen wasp's abdomen contained extensive fat bodies partially obscuring the visceral tracheal trunks.

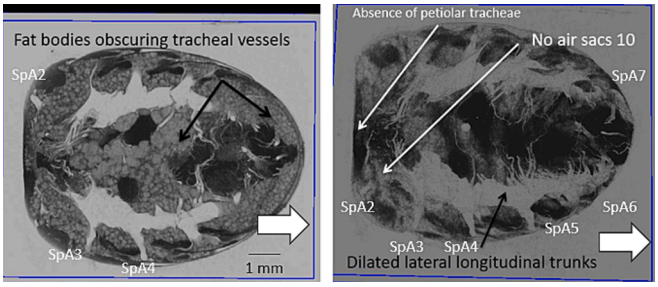

Fig. 8b. On the left is an inverted 3-D dorsal cut plane view of the abdomen of PreQW8 showing no evidence of petiolar tracheal trunks and the absence of abdominal air sacs (10). On the right is the same view after using Level/Window settings to mask out the fat bodies and improve the visibility of the visceral tracheal trunks. The entry points of abdominal spiracles A2-A7 are shown. Both images show a more dilated lateral longitudinal tracheal trunks than seen in the other 29 wasps.

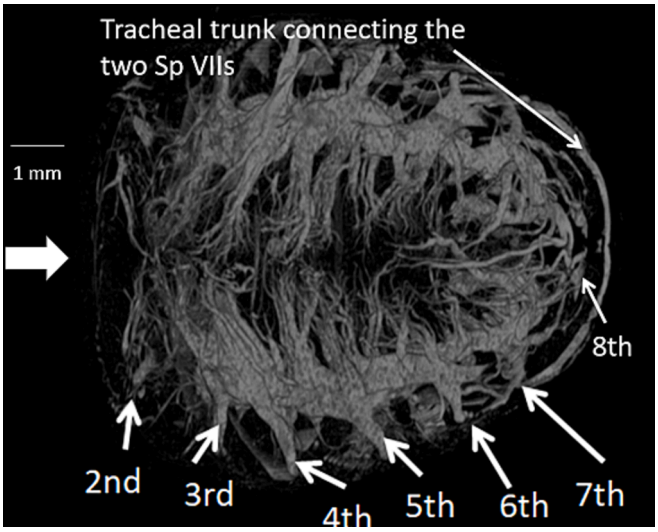

Fig. 9. Inverted 3-D volume view of the entire intra-abdominal tracheal system of PreQW 8. All 8 spiracular tracheae are identified including the two Sp VIIIs which were hidden within the sting recess. No connecting tracheal vessels were detected in the petiole and abdominal air sacs 10 were absent. The two lateral longitudinal tracheal trunks were dilated and there was an extra tracheal trunk connecting the two Sp VIIs that was not detected in any of the other 29 wasps.

Fig. 2b) we used Tomomask (http/tomomask.com: Greco et al., 2014, Bell et al., 2021; Bell et al., 2022) to select either the transverse 2-D sections representing the abdominal half of the wasp or the rest of the insect representing its thorax and head. We found that the most convenient dividing point was the midpoint of the thin wasp 'waist' or Petiole through which the two relatively large tracheal vessels connect the thoracic and abdominal systems (see arrows on Fig. 1 and Fig. 2). The two halves of each wasp scan were then reconstructed in both Disect (Fig. 3a) and Tomomask. We resaved both the abdominal and head + thorax sections of each wasp scan using Tomomask's invert facility so that the X-ray attenuation values of each individual voxel within the datasets was inverted from values ranging from 0–255 to 255–0. As can be seen in Fig. 3a and Fig. 3b this meant that the surrounding air and internal air-filled structures such as air sacs, tracheal vessels, and gas within the gastrointestinal tract (especially that contained in the crop) became white whereas all other internal insect structures with X-ray attenuation values greater than that of air such as the exoskeleton, skeletal muscle, viscera etc showed up as varying shades of grey.

When the datasets attenuation values were initially inverted the default Level and Windows settings in Disect were 128/256 (Fig. 3a). We

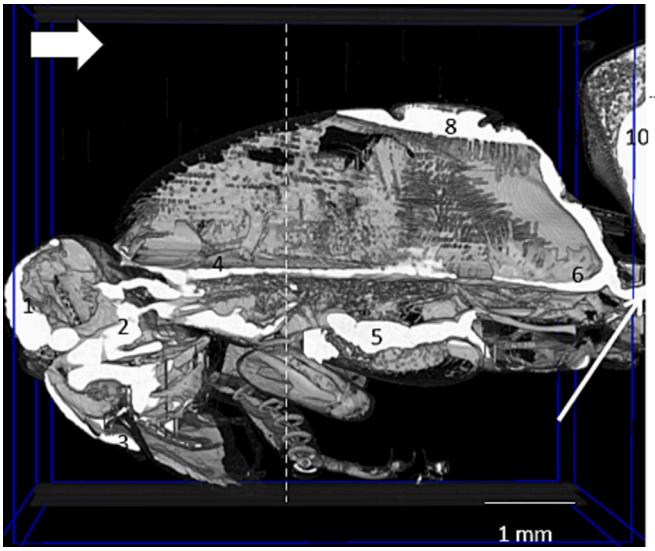

Fig. 10a. A 3-D cut plane parasagittal view of the head and thorax of PreQW 1 after inversion of the attenuation values and removal of surrounding air. The two large tracheal trunks passing through the petiole and connecting the abdominal and thoracic tracheal systems were easily visible (white arrow) and connected to multiple air sacs and tracheal vessels arising from the two thoracic spiracles (T2 and T3) as well as that in the propodeum. The air sacs labelled 1, 2, 3, 5, 6, 8 and 10 correspond with those in similar positions described in the honeybee by Snodgrass (Fig. 1a/1b). The dashed white line shows the position of the transverse cut-plane view in Fig. 10b.

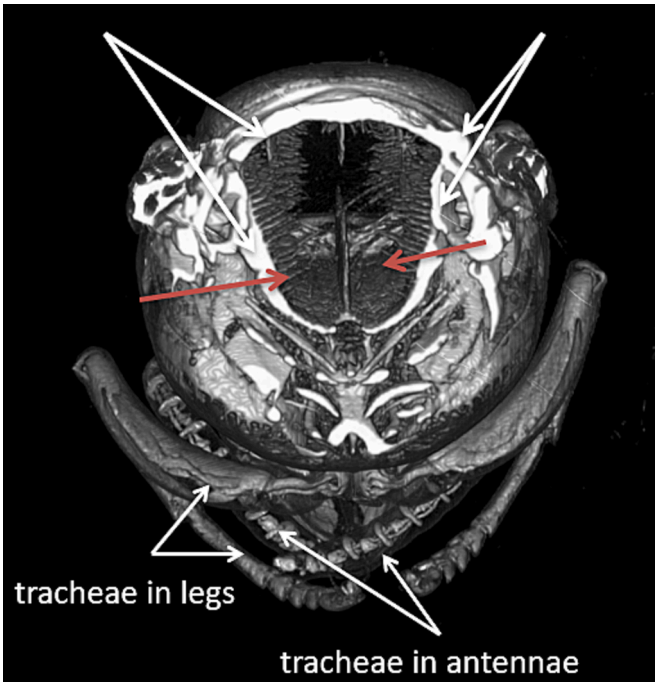

Fig. 10b. A transverse mid-thoracic 3-D volume cut-plane inverted image of PreQW 1. The two large indirect wing depressor muscles are surrounded by air sacs (white arrows) from which multiple delicate tracheal vessels can be seen penetrating between the flight muscle fibres (red arrows). Tracheae in the legs and antennae are also visible. The ring-like air spaces in the antennae are an artifact due to air spaces in-between the individual antennomeres. Similar ring-like air space artifacts are seen in the antennae in Fig. 11a and Fig. 11b.

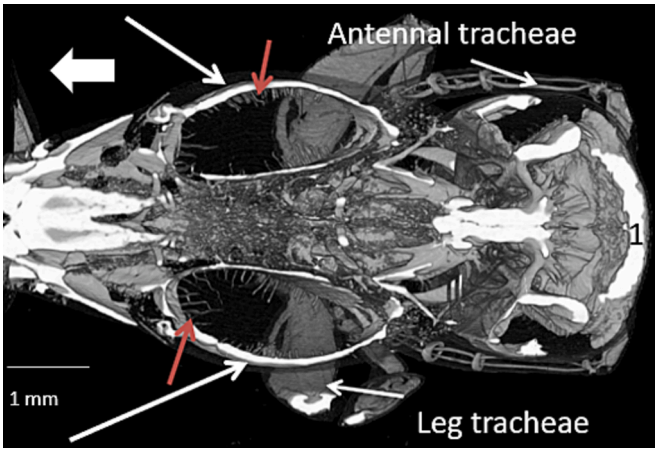

Fig. 11a. A dorsal cut-plane 3-D inverted view of the head and thorax of PreQW1. The white arrows show the air sacs surrounding the two indirect dorso-ventral flight muscles responsible for elevating the wings. These air sacs give off multiple delicate tracheae passing centrally between individual muscle fibres (red arrows). Also visible are head sac 1 and tracheal vessels in both the legs and antennae.

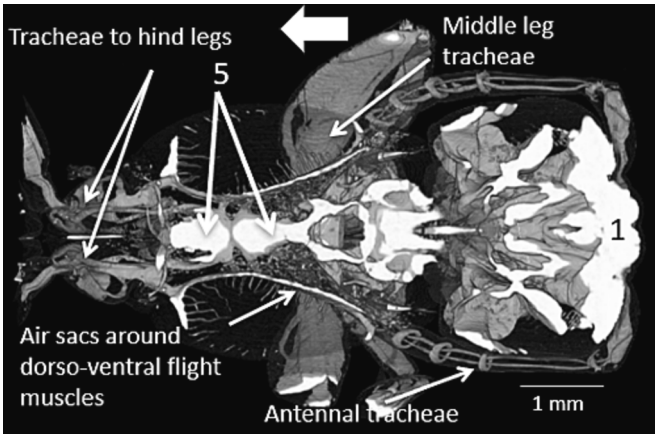

Fig. 11b. A more ventral, dorsal cut-plane 3-D inverted view of the head and thorax of PreQW 1. This is at the level of the single centrally placed air sac labelled as 5 in Fig. 10a. It supplies the tracheae running to all 3 pairs of legs, the air sacs surrounding the dorso-ventral flight muscles and then runs into the head.

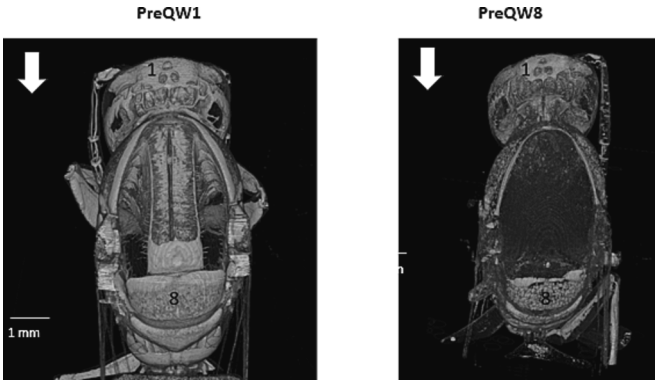

Fig. 12a. On the left is an inverted 3-D dorsal view of the thorax and head of PreQW 1 with normal air sacs and tracheae. On the right is a similar view of PreQW 8 showing a relative paucity of tracheal vessels and air sacs.

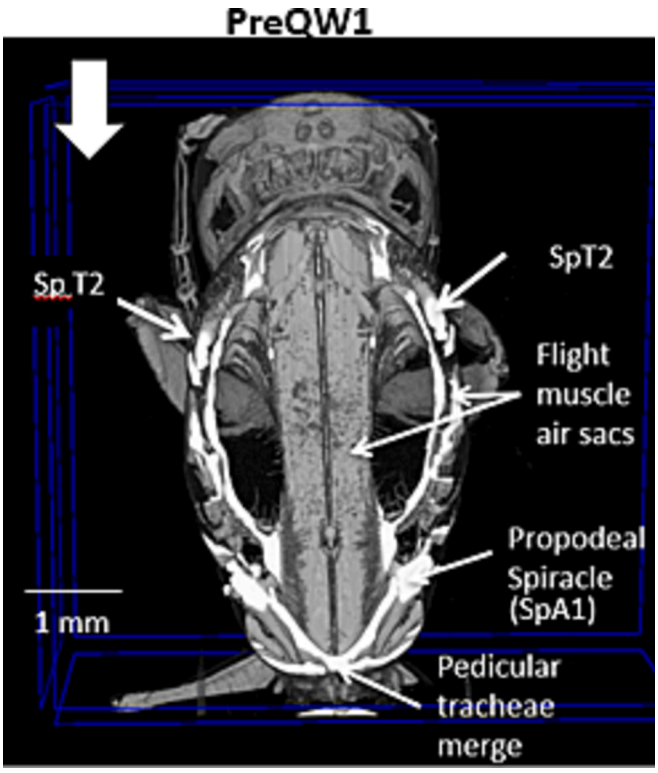

Fig. 12b. Dorsal cut-plane 3-D views of the thorax and head of PreQW1 at the level that the spiracular tracheae of T2 commences (white arrows). The air sacs surrounding the two medially situated indirect flight muscles running the length of the thorax and the more lateral dorso-ventral indirect flight muscles are shown.

found that by further adjustment of the Level and Window setting as shown in Figs. 3b and 3c, better definition of the tracheal structures could be obtained.

The exact figures varied slightly between different scans but Level/Width values of about 255/74 proved optimal for viewing 3-D cut-planes and 255/255 proved most satisfactory for studying 2-D slices using the Multi-Planar Reconstruction facility (MPR). It proved relatively simple to use the MPR (multi planar format) facilities that Disect and Tomomask possess to work out which of the larger tracheal trunks connected to each other and to what significant sized air sacs (see Figs. 4a and 4b).

Since the consensus was that the tracheal system of the abdomen was simpler and more akin to that of the larval stages (Vinal, 1919; Snodgrass, 1956; Chapman, 1998; Klowden, 2007), we studied the intra-abdominal tracheal system first (see Fig. 3-6). In several of the wasps we also used the 3-D paint software that is freely available from Microsoft Ltd to convert from white to black any whiteness due to air surrounding the insect (see Figs. 7a and 7b). This meant that the entire insect's respiratory system could be viewed. This included any air sacs situated immediately below its exoskeleton. This process was somewhat time consuming and labour intensive as it involved a single transverse by transverse slice approach to build up the 3-D volume views shown in Fig. 7b. This approach was slightly more problematic in the abdomen because the overlapping tergae and sternae often had air trapped between them (Fig. 8a) and there was also the additional problem of air within the sting recess.

2.5. Labelling of thoracic and abdominal spiracles and main tracheal trunks

Several factors influenced our attempts to identify and correctly label individual spiracles arising in either the thorax or abdomen of the wasp.

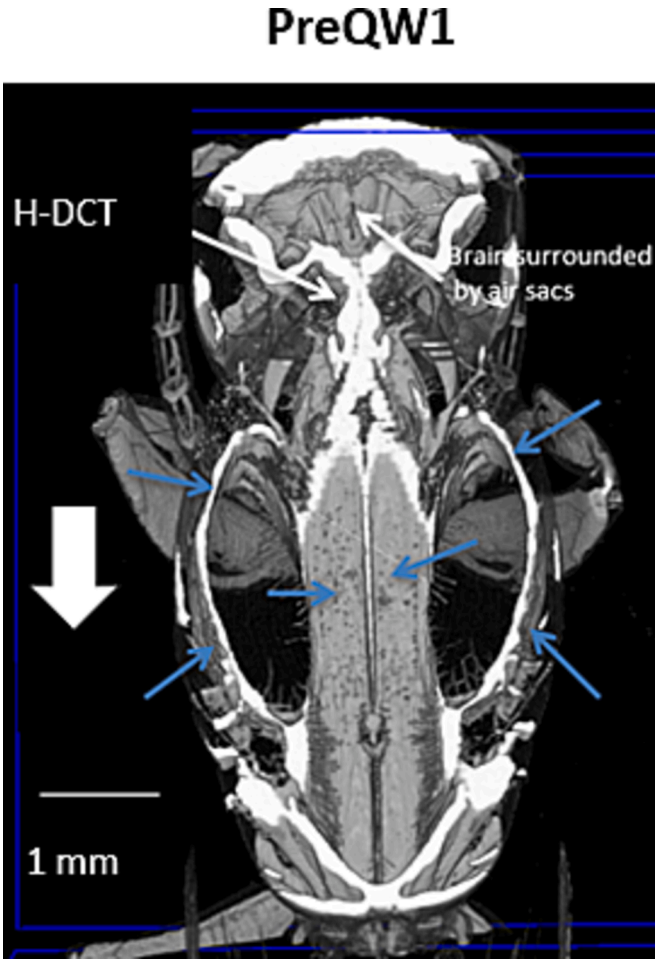

Fig. 12c. Dorsal cut-plane 3-D view of the thorax and head of PreQW1 at the level that the upper pair of tracheal trunks that arise from spiracular trachea T2 (SpT2) and pass through the neck and into the head (labelled as H-DCT). The brain is surrounded by head air sacs. The well- developed air sacs surrounding the indirect flight muscles (blue arrows) of the normal wasp were absent in PreQW8 (not shown).

These included knowing that no extant insect has a spiracle arising from its prothorax (Herhold et al., 2023) and thus the first thoracic spiracle rather than being 'T1′ and labelled Sp1 by Snodgrass in Fig. 1b is T2. Similarly, the spiracle arising in the metathorax is more correctly T3 and not T2 (Herhold et al., 2023). In addition, in Hymenoptera such as wasps, bees, and ants, the first abdominal segment is joined to the thorax as the propodeum.

This means that the first abdominal spiracle appears to arise in the thorax (and might thus be erroneously labelled as T3 but is A1). The wasp waist or Petiole is the second abdominal section and its abdominal spiracle is more correctly A2 and not A1. We have also elected when certain larger tracheal trunks are identified, such as those passing though the neck to the head (but arising from the most anterior thoracic spiracle T2), to use the new tracheal nomenclature system recommended by Herhold et al., 2023 in pages 22–27 of their paper.

3. Results

All 31 wasps were successfully scanned. One of the pre-hibernation queen's scans (preQW6) was clearly highly abnormal and was excluded (Bell et al., 2023). Thus, we were left with eight pre- hibernation queen wasps, 12 post-hibernation queen wasps and ten worker wasp scans to analyse.

As we showed in our previous paper (Bell et al., 2023), there were

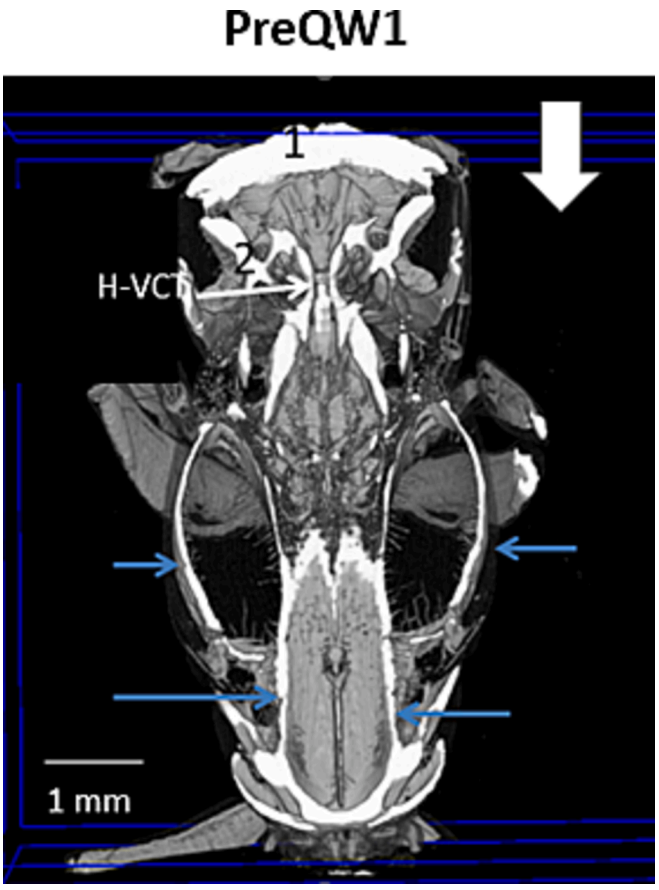

Fig. 12d. Dorsal cut-plane 3-D view of the thorax and head of PreQW1 at the level that the lower two pairs of tracheal vessels enter the head via the neck (labelled as H-VCT). These two tracheae arise in the single centrally placed air sac shown in Fig. 13a. The well-developed air sacs surrounding the indirect flight muscles in PreQW1 (blue arrows) were not seen in PreQW8.

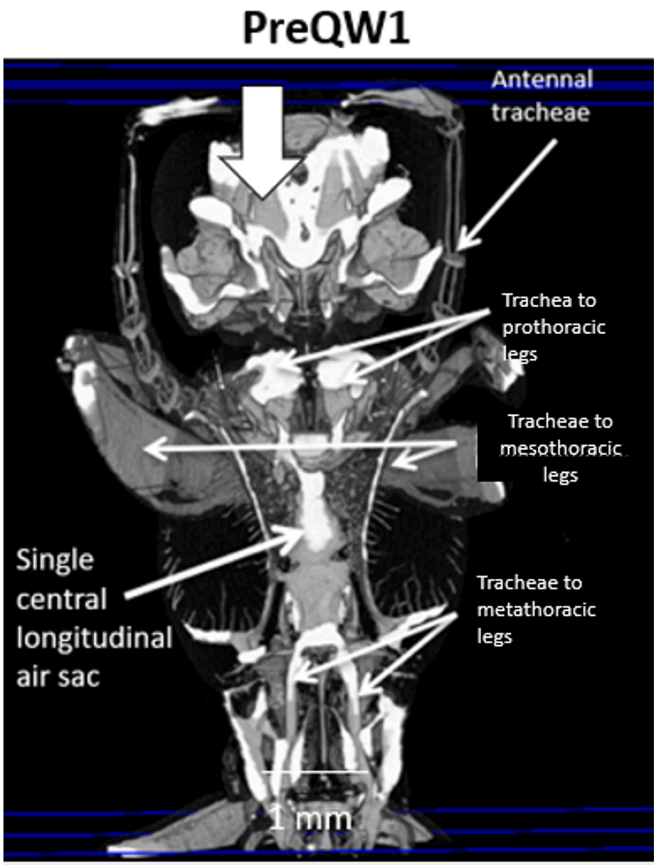

Fig. 13a. Dorsal cut-plane 3-D view of the thorax and head of PreQW1 at the level of the single large central longitudinal thoracic air sac. This supplies the legs, communicates anteriorly with the lower of the two pairs of tracheal vessels passing into the head and communicates posteriorly with both the tracheal vessels arising from the propodeal spiracles, and those passing via the pedicle into the abdomen.

significant differences in the intra- abdominal fat content of the pre hibernation queen wasps compared with either the post hibernation wasps or the female worker wasps. However, in terms of their respiratory systems, we could not discern any obvious differences and so the groups were combined. We thus had the respiratory systems of 20 queen wasps and 10 smaller female worker wasps to analyse and compare with those of the honeybee (Figs. 1a and 1b). This was done initially in relation to their relatively simple intra-abdominal tracheal systems before attempting to analyse the more complex system of the thorax and head which contained many more air sacs.

3.1. Queen wasps' and worker wasps' abdominal tracheal systems

In 19/20 of the queen wasps and all 10 of the worker wasps the two large tracheal trunks passing through the petiole were clearly seen expanding almost immediately into the 2 large abdominal air sacs designated by Snodgrass in the honeybee as air sacs 10. These two air sacs also receive air via abdominal spiracle II and III. Abdominal spiracles III to VII, or at least their spiracular trunks on both sides, could be discerned feeding into the interconnected two main lateral longitudinal trunks (Figs. 3 and 4). Coming off these lateral longitudinal trunks, other tracheal vessels could be identified. These passed dorsally and ventrally as well as relatively horizontally to the viscera (Fig. 5 and 6). The two abdominal spiracles VIII could be seen within the sting recess with the two spiracular trunks anastomosing with the rest of the trachea connecting spiracles III to VII. (Fig. 5b). No abdominal air sac was seen in the position indicated by Snodgrass in the honeybee as air sac 9.

One queen wasp (designated as pre-hibernation queen wasp 8 or PreQW) was clearly different from The remaining 29/30 wasps in having no discernible petiolar tracheal trunks connecting the Abdominal respiratory system with that of the thorax and head. There was no evidence for the large Proximal air sacs identified as abdominal sacs 10. Abdominal spiracular trunks II-VIII could all be seen as could the two lateral somewhat dilated lateral longitudinal connecting trunks with branches passing dorsally, ventrally and to the viscera (Figs. 8b and 9). In addition, there was a relatively large tracheal anastomotic trachea connecting the two spiracle VIIs (Fig. 9). Such a vessel was not seen in any of the remaining 29 queen wasps or 10 worker wasps.

3.2. Queen wasp and worker wasp thoracic and head tracheal systems

In 19/20 of the queen wasps and all 10 worker wasps the two petiolar tracheal trunks connecting with the two large proximal abdominal air sacs (designated 10 by Snodgrass) could be seen passing forward into the thorax and connecting with other intra-thoracic tracheae and air sacs (Fig. 10a). No such petiolar tracheal trunks could be detected in PreQW8 in keeping with the intra-abdominal findings described above. The spiracular trunks of thoracic spiracle T2 led into large tracheal vessels and (inter alia) passed forward through the neck and into the head. These were easily visualised and followed. Thoracic spiracle T3 was small and only occasionally identified. In contrast, the propodeal spiracle (i.e., abdominal spiracle A1) was much easier to visualise and the course of its various tracheal branches and connecting air sacs were easily traced.

Although intra-thoracic air sacs were seen in the mesoscutellum

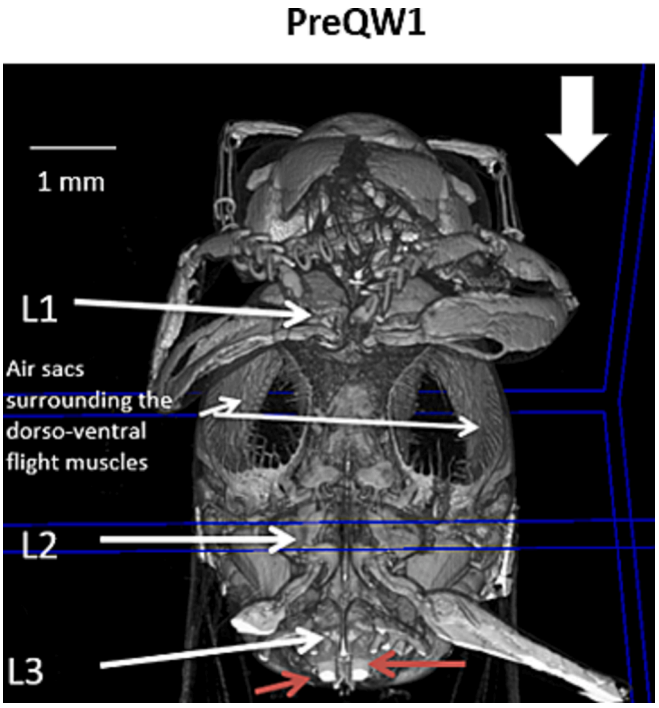

Fig. 13b. Ventral 3-D volume view of the thorax and head of PreQW1. The tracheae within the prothoracic, mesothoracic and metathoracic legs were poorly developed in PreQW8 (not shown). The two tracheal trunks passing through the pedicle from the abdomen in PreQW1(red arrows) were absent in PreQW8 (not shown). The air sacs surrounding the dorso-ventral flight muscles, with their fine tracheae passing into the centres of the muscles between individual muscle fibres, were well seen.

Fig. 14a. External Inverted 3-D frontal view of the head of PreQW1. The frontal and mandibular air sacs are shown (white arrows) as are the tracheae in the antennae and prothoracic legs.

region and sides of the propodeum in similar positions to those described by Snodgrass in the honeybee as air sac 8 and 7 respectively (Figs. 1 and 2), other air sacs such as those he designated as air sacs 4, 5 and 6 were not so obvious in the same positions in the wasp. It was frequently difficult to distinguish between what was a rather dilated flattened tracheal trunk or alternatively a small thin flat intrathoracic air sac. It could however be clearly seen that the two pairs of large indirect flight muscles were surrounded by air sacs that also had thin tracheal vessels passing into the muscles themselves (Figs. 10b, 11a,11b, 12b, 12c, 12d, 13a and 13b). Relatively large tracheal vessels and small air sacs were also seen near the sites where direct flight muscles and muscles to the pro, meso and metathoracic legs were situated. There was a single midline linearly placed air sac in the lower thorax in roughly the position of the air sac designated as 5 by Snodgrass (see Figs. 1b, 10a, 11b and 13a). However, this appeared more like that described in Drosophila as the parenteric sac by Miller (1950) and which was seen to connect with the two petiolar tracheae and both T2 and T3 as well as A1. Tracheal vessels from this centrally placed air sac supplied all 3 sets of legs as well as passing forwards and upwards through the lower neck and into the head. There were 2 pairs and not simply the one pair of tracheal vessels arising from Thoracic Spiracle 2 as described by Snodgrass (Figs. 1a, 1b, 12c, 12d, 15b, and 16).

The air sacs we delineated in the wasp heads were in approximately the same places as those described by Snodgrass as air sacs 1,2 and 3 (see Figs. 1a and 1b) which are situated (a) against the upper part of the face and covering the top of the brain, (b) lying against the base of the compound eye and above the optic lobe and (c) one situated above the base of the mandible respectively (Fig. 14a, 14b, 14c, 15a, 15b, and 16). As in the thorax and abdomen, the tracheal system in the head was considerably more complicated than that described by Snodgrass. For example, there were significant sized air sacs surrounding both the large mandibular adductor and somewhat smaller abductor muscles (not shown) and the infrabuccal sac or gnathal pouch (Fig. 16).

The Queen pre-hibernation wasp 8, that had no trace of petiolar tracheal trunks, had a highly abnormal intrathoracic tracheal system. The air sacs surrounding the indirect flight muscles of PreQW8 were reduced in size and extent compared to any of the other 29/30 wasps. Tracheal vessels supplying the mesothoracic legs were virtually non-existent. In contrast in preQW8 head air sacs were relatively normal compared with all 29/30 of the remaining wasps.

4. Discussion

We have demonstrated in 30 wasps how detailed visualisation of the insect respiratory system can be achieved quickly and relatively simply by inverting the X-ray attenuation values obtained using micro-CT scanned specimens stored and analysed as 8-bit data. Since completing this study, the recently published paper from the American Museum of Natural History (Herhold et al., 2023) has convinced us that had we used 16-bit data and a software package such as 'Slicer' (Fedorov et al., 2012), inverting the data sets from black and white to white and black might not have been necessary. We found that in most cases, it was not necessary to go through the laborious and time- consuming process of removing, on a transverse slice by slice basis, the white background due to air surrounding the specimen (Figs. 7a and 7b). Although removing background air manually did improve image quality (Figs. 7b, 9), accurate anatomical definition of the respiratory system was still possible without this extra labour-intensive step. Using a combination of the software tools that come with most micro-CT systems including 2-D transverse, coronal and sagittal sections combined! with multiplanar views, it was possible to follow individual tracheal trunks or air sacs to delineate connections and identify which internal structures were being supplied by what trachea (Figs. 4a and 4b). These results could be confirmed in most cases using 3-D cut-plane views (Figs. 3a, 3b, 3c, 5a,

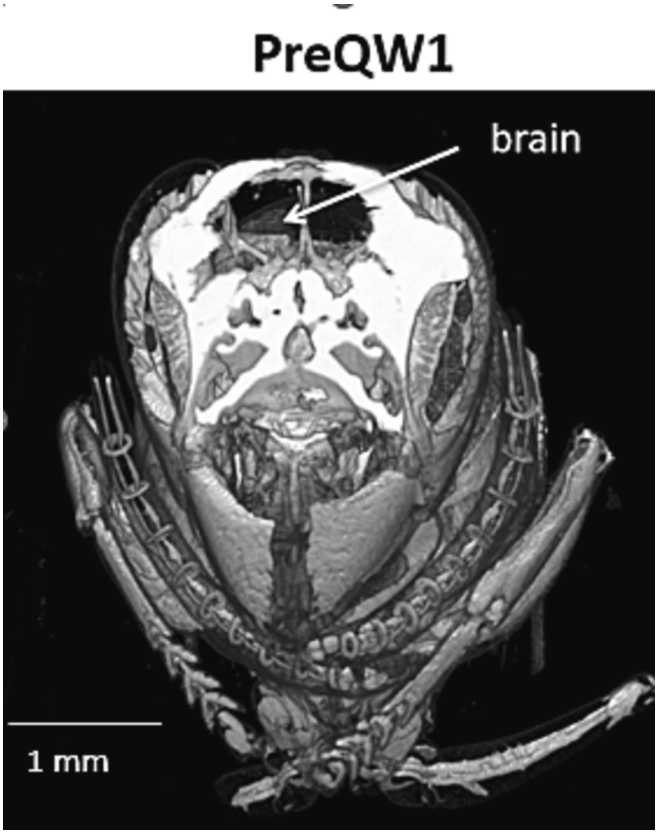

Fig. 14b. Inverted 3-D frontal cut-plane view of the head of PreQW1. The air sacs surrounding the brain (white arrow) are seen.

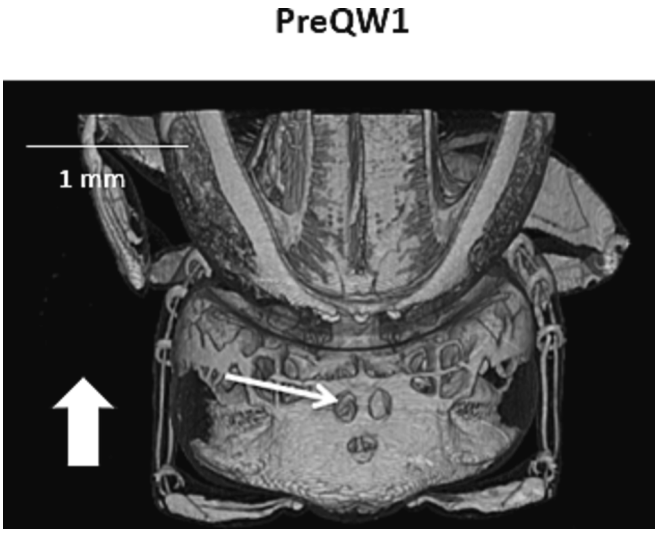

Fig. 15a. Inverted dorsal external 3-D volume view of the head and neck regions of PreQW1. There are three holes in the frontal air sacs covering the upper surface of the brain through which the median and two lateral ocelli pass (white arrow).

5b and Fig. 6) without needing to remove surrounding air (Figs. 7a and 7b). Air removal would of course be required if measuring tidal volumes or to produce an STL file for 3-D printing (Greco et al., 2014).

The importance of altering the X-ray attenuation values by adjusting the Window and Level settings where necessary is illustrated in Figs. 3b and 8b.

Using Snodgrass's published diagrams of the tracheae and air sacs of

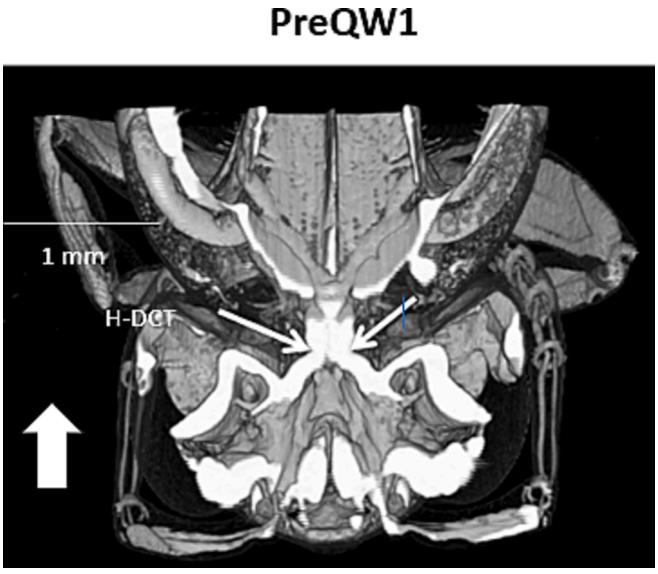

Fig. 15b. 3-D volume dorsal cut-plane view of the head and neck regions of the heads of PreQW1 taken at the level that the upper of the two pairs of tracheal vessels that supply the head (white arrows labelled H-DCT).

the adult honeybee (Figs. 1a and 1b) as a guide to our own study of the wasp proved helpful. We also made use of the more recent, well-illustrated book by Stell (2012) on bee anatomy. Stell, a surgeon by profession, performed intricate dissections of the bee's head air sacs which look remarkably like those in Fig. 15a of the 'holes' surrounding the three ocelli of the wasp. As expected, wasps, like bees and ants, have 3 rather than the usual two spiracles on each side of their thoraxes because the first abdominal section or propodeum and its propodeal spiracles have become an intimate part of the thorax. In 29/30 of the specimens studied there were, as described by Snodgrass (1954) and Stell (2012), two relatively large and easily visualised petiolar tracheal trunks connecting the respiratory systems of the abdomen with that supplying the thorax and head. As previously shown (Bell et al., 2023), the size of the two large abdominal air sacs, designated number 10 by Snodgrass, were quite variable depending on such factors as the amount of fluid in the wasp's crop as well as the quantity of abdominal fat. Nevertheless, they were a constant finding in 29/30 of the wasps. The development of the tracheal system is under genetic control, and we suspect that the highly abnormal tracheal system of Pre-hibernation Queen 8 was due to a genetic abnormality (Figs. 8a, 8b, 9).

We found no evidence of the small single abdominal air sac designated number 9 by Snodgrass (Fig. 1a) in any of our 30 wasps. All had two and not one pair of tracheal vessels passing from the thorax through the neck and into the head (see Figs. 12c, 12d, 15b, and Fig. 16). These we designated as H-DCT (head dorsal cephalic trunk and H-VCT (head ventral cephalic trunk) in keeping with the new nomenclature suggested by Herhold et al. (2023). We demonstrated that the entire interconnecting tracheal system of the wasps was considerably more complex than that previously illustrated. This extra detail allowed us, for example to delineate the air sacs surrounding the Gnathal sac (Fig. 16) and we postulate that their periodic expansion may in part explain the mechanism by which this structure is periodically emptied (Duncan, 1939, Spradbery, 1973). Whilst developing our method using inversion of attenuation values, we watched a Bruker Ltd webinar lecture on the use of micro-CT in insects by Professor Alba-Tercedor (https://www.bruker.com/en/news-and-events/webinars/2021/Experiences-in-The-Use-of-Micro-CT-in-Insect-Research.html). He described a similar method of delineating the tracheal system of insects by inverting the X-ray attenuation values of 8-bit data. We are not aware of any published data from Professor Alba-Tercedor's group. Had this group used 16-bit rather than 8-bit data the inversion of X-ray attenuation values would probably have

Fig. 16. 3-D cut-plane midline sagittal view of the head and neck region of PreQW1. The upper and lower pairs of tracheal vessels supplying the head are shown and labelled as H-DCT and H- VCT (white arrows). The upper and lower dotted lines indicate the level of the dorsal cut-plane views shown in 15a and 15b. The red arrow points to the Gnathal sac.

been unnecessary.

Herhold et al. (2023) state that they found in their 4-year study that it was preferable to store the insect specimens at −80 degrees rather than at −20 degrees. This is because at higher temperatures fluid was more likely to leak into the smaller tracheal vessels and obscure their visualisation on micro-CT. We initially stored our samples in a domestic freezer at −20 degrees prior to transfer for storage in our university's deep freezer at −80 degrees but intend in future studies to keep our insects alive until it is possible to euthanise them at −80 degrees. This is likely to be particularly important when studying the tracheal systems of very small adult insects such as Drosophila which are often less than 3 mm in length.

Most studies on the effects of genetic manipulation and control of the tracheal system of insects have been performed in the fruit fly and have mainly concerned embryogenesis and tracheal development at a larval stage (Hayashi and Kondo, 2018). Genetic-related imaging studies have been successfully carried out in adult wasps (Harrop et al., 2020, Crowley et al., 2021). Advances in Micro-CT analysis methods to delineate the tracheal system might usefully advance studies of tracheal development in more genetically defined albeit smaller insects.

5. Conclusion

We report a relatively simple method using X-ray micro-CT to accurately delineate the entire tracheal system of 30 adult Vespula vulgaris wasps (20 queen wasps and 10 worker). We have compared our findings with previously published work performed on the tracheal system of the honeybee. In reporting our findings, we have used the newly published tracheal nomenclature system developed at the American Museum of Natural History. We show that the tracheal system of this wasp is broadly similar, but considerably more complex than that suggested by drawings of dissected honeybee specimens. One of the 30 wasps had a markedly different tracheal system from the other 29 wasps, and we suspect this is a genetic variant. There is considerable interest in the genetic control and development of the tracheal system with most of the work to date having been performed during either embryogenesis or the larval stages of the fruit fly. Far fewer tracheal-related studies have been performed during either pupariation or in adult insects in part because of the difficulties relating to dissecting out the tracheal system. Micro-CT methods might usefully define the tracheal systems of other adult insect species and anatomical changes arising from genetic alterations.

Declaration of Competing Interest

The authors declare that they have no known competing financial interests or personal relationships that could have appeared to influence the work reported in this paper.

Data availability

Data will be made available on request.

Acknowledgements

We are grateful to Dr Gavin Broad from the Natural History Museum in London for his helpful suggestions. The paper was greatly improved by comments and corrections from the journal's reviewers and editor.

Author statement

Bell conceptualised this study and sourced the insects for study. Corps, Mortimer, Gretton and Bell worked to develop software and obtained the imaging studies. Bell analysed the data. Bell and Connett developed drafts of the manuscript. All authors edited the manuscript and Connett finalised all documents.

References

Alba-Tercedor, J., 2021. https://www.bruker.com/en/news-and-events/webinars/2021/Experiences-in-The-Use-of-Micro-CT-in-Insect-Research.html.

Bell, G.D., Woolnough, L., Mortimore, M., Corps, N., Hudson, D.M., Greco, M.K., 2012. A preliminary report on the use of benchtop x-ray micro-computerised tomography to study the malpighian tubules of the overwintering seven spotted ladybird *Coccinella septempunctata* L.(Coleoptera: Coccinellidae). Psyche, 348348: 1.

Bell, G.D., Bury, N., Woolnough, L., Corps, N., Mortimore, D.B., et al., 2020. Use of micro-computed tomography to study the moult cycle of the freshwater amphipod Gammarus pulex. Zoology 143, 125833.

Bell, G.D., Broad, G.R., Corps, N., Mortimer, D., Gretton, S., Bury, N., 2023. Visualising fat reserves in an insect: A method using X-ray micro-computerised tomography of the Common Wasp (Vespula vulgaris). Zoology 158, 126092. ISSN 0944–2006.

Bell, G.D., Bury, N., Gretton, S., Mortimore D.B. et al. (2021) An X-ray micro-computer study of the Malpighian tubules of the developing Blue Bottle fly (*Calliphora vomitosia*) Diptera: Calliphoridae. Zoology 149 (2021) 149 1259.

Chapman, R.F., 1998. The Insects: Structure and Function, 4th ed. Cambridge University Press, Cambridge, UK.

Crowley, L., 2021. The genome sequence of the common wasp, *Vespula vulgaris* (Linnaeus, 1758). Wellcome Open Res. 6, 232.

Duncan, D.C. (1939) A contribution to the biology of North American vespine wasps. Stanford University Publications, University Series, Biological Sciences, 8(1), Oxford University Press, Oxford, 1-257.

Fedorov, A., Beichel, R., Kalpathy-Cramer, J., Finet, J., Fillion-Robin, J.-C., Pujol, S., Bauer, C., Jennings, D., Fennessy, F., Sonka, M., Buatti, J., Aylward, S., Miller, J.V., Pieper, S., Kikinis, R., 2012. 3d slicer as an image computing platform for the quantitative imaging network. Magn. Reson. Imaging 30 (9), 1323–1341.

Friedrich, F., Beutel, R.G., 2008. Micro-computer tomography and a renaissance of insect morphology. Proc. SPIE 7078 (September 2016), 70781U.

Greco, M.K., Tong, J., Soleimani, M., Bell, D., Schäfer, M.O., 2012. Imaging live bee brains using minimally invasive diagnostic radioentomology. J. Insect Sci. 12 (89), 1–7.

Greco, M.K., Bell, G.D., Woolnough, L., Laycock, S., Corps, N., et al., 2014. 3-D visualisation, printing, and volume determination of the tracheal respiratory system in the adult desert locust, Schistocerca gregaria. Entomol. Exp. Appl. 152, 42–51.

Greenlee, K.J., Henry, J.R., Kirton, S.D., Westneat, M.W., et al., 2009. Synchrotron imaging of the grasshopper tracheal system and physiological components of tracheal hypermetry. Am. J. Physiol. 297, 1343–1350.

Harrop, T.W.R., Guhlin, J., McLaughlin, G.M., Permina, E., Stockwell, P., Gilligan, J., Le Lec, M.F., Gruber, M.A.M., Quinn, O., Lovegrove, M., Duncan, E.J., Remnant, E.J., Van Eeckhoven, J., Graham, B., Knapp, R.A., Langford, K.W., Kronenberg, Z., Press, M.O., Eacker, S.M., Wilson-Rankin, E.E., Purcell, J., Lester, P.J., Dearden, P.K., 2020. High-quality assemblies for three invasive social wasps from the Vespula genus. G3 Genes|Genomes|Genetics 10 (10), 3479–3488.

Hartung, D.K., Kirton, S.D., Harrison, J.F., 2004. Ontogeny of tracheal system structure: a light and electron-microscopy study of the metathoracic femur in the American locust *Schistocerca americana*. J. Morphol. 262, 800–812.

Hayashi, S., Kondo, T., 2018. (2018) Development and Function of the Drosophila Tracheal System. Genetics 209 (2), 367–380. https://doi.org/10.1534/genetics.117.300167.

Herhold, H.W., Davis, S.R., Degrey, S.P., Grimaldi, D.A. (2023) comparative anatomy of the insect tracheal system Part 1: Introduction, Apterogotes, Paleoptera, Polyneoptera. Bulletin of the American Museum of Natural History Number 459,184 pp.,122 figures, 5 tables,78 plates. Issued March 10, 2023.

Iwan, D., Kamiński, M.J., Raś, M., 2015. The last breath: A micro-CT -based method for investigating the tracheal system in hexapoda. Arthropod Struct. Dev. 44, 218–227.

Kaiser, A., Klok, C.J., Socha, J.J., Lee, W.-K., Quinlan, M.C., Harrison, J.F., 2007. Increase in tracheal investment with beetle size supports hypothesis of oxygen limitation on insect gigantism. PNAS 104 (32), 13198–13203.

Kirkton, S.D., Hennessey, L.E., Duffy, B., Bennett, M.M., Lee, W.-K., Greenlee, K.J., 2012. Intermolt development reduces oxygen delivery capacity and jumping performance in the American locust (*Schistocerca americana*). J. Comp. Physiol. B 182 (2), 217–230.

Klowden, M.J., 2007. Physiological Systems in Insects, 2nd edn. Elsevier, Amsterdam, The Netherlands.

Meyer, E.P., 1989. Corrosion casts as a method for investigation of the insect tracheal system. Cell Tissue Res. 256, 1–6.

Miller, A. (1950) Chapter entitled The Internal Anatomy and Histology of the Imago of Drosophila melanogaster. In Biology of Drosophila Ed Demerec, M. pp 420-534. Facsimile Edition Copyright Cold Spring Harbor Laboratory press 1994.

Shaha, R.K., Vogt, J.R., Han, C.-S., Dillon, M.E., 2013. A micro-CT approach for determination of insect respiratory volume. Arthropod Struct. Dev. 42 (5), 437–442.

Snelling, E.P., Seymour, R.S., Runciman, S., Matthews, P.G.D., White, C.R., 2012. Synmorphosis and the insect respiratory system: a comparison between flight and hopping muscle. J. Exp. Biol. 215, 3324–3333.

Snodgrass, R.E., 1956. Anatomy of the honeybee. Comstock Pub. Assoc., Ithaca, New York, p. 352.

Socha, J.J., Förster, T.D., Greenlee, K.J., 2010a. Issues of convection in insect respiration: Insights from synchrotron x-ray imaging and beyond. Respir. Physiol. Neurobiol. 173, S65–S73.

Socha, J.J., Forster, T.D., Greenlee, K.J., 2010b. Issues of convection in insect respiration: insights from synchrotron X-ray imaging and beyond. Respir. Physiol. Neurobiol. 173S, S65–S73.

Spradberry, J.P., 1973. An account of the biology and natural history of social and solitary wasps. University of Washington Press, Seattle, p. 408.

Stell, I., 2012. Respiratory System. Chapter in Understanding Bee Anatomy. The Catford Press. McGraw Hill, New York, NY, USA, pp. 154–162.

Sumner, S., 2022. Endless Forms: the secret world of Wasps. William Collins.

Tam, M., Bell, G.D., Williams, S., Heylings, D., 2007. Making cross sectional anatomy an accessible adjunct for anatomy education. Clin. Anat. 20, 465–472.

Tarplee, M., and Corps, N. (2008) Skyscan 1072 Desktop X-Ray Microtomograph – Sample Scanning, Reconstruction, Analysis and Visualisation (2-D & 3-D) Protocols. Guidelines, Notes, Selected References and FAQ. Available at: http://www.geog.qmul.ac.uk/docs/staff/4952.pdf (accessed May 2008).

Thielens, A., Bell, G.D., Mortimore, D.B., Greco, M.K., et al., 2018. (2018) Exposure of Insects to Radio Frequency Electromagnetic Fields from 2 to 120GHz. Sci. Rep. 8, 3924.

Vinal, S.C., 1919. The respiratory system of the Carolina locust (*Dissosteira carolina* Linne). J. New York Entomol. Soc. 27, 19–32.

Westneat, M.W., Betz, O., Blob, R.W., Fezzaa, K., et al., 2003. Tracheal respiration in insects visualised with synchrotron X-ray imaging. Science 299, 558–560.

Wigglesworth, V.B., 1950. A new method of injecting the trachea and tracheoles of insects. Q. J. Microsc. Sci. 91, 113–137.